Journal of Statistical Physics, Vol. 43, Nos. 3/4, 1986

The Two-Dimensional ANNNI Model in the CVM Approximation

Alphonse Finel[1,2] **and Didier de Fontaine**[1]

Received October 14, 1985

The phase diagram of the two-dimensional ANNNI model is investigated by the cluster variation method (CVM). We confirm the stability of the disordered phase down to $T=0$ and the absence of a Lifshitz point at finite temperature for $K<\frac{1}{2}$, where K is the ratio of the second to the first neighbor pair interactions. Two different modulation regimes for the correlation functions of the disordered phase are separated by a "disorder" line along which the q vector of the susceptibility maximum undergoes a lock-in transition. The study in reciprocal space of the stability of the disordered phase allows us to define a critical line in the phase diagram along which the q vector characterizing the instability is incommensurate. Finally, we show the existence of another Lifshitz point for K tending to infinity.

KEY WORDS: ANNNI model; floating phase; two-dimensional Ising model.

1. INTRODUCTION

Ising models with competing interactions between nearest and next-nearest neighbors in one direction (Axial Next-Nearest-Neighbor Ising, or ANNNI, model) have been studied extensively because of the simplicity of their Hamiltonians and the variety of physical features they display; for a recent review see Ref. 1.

The ANNNI model in a simple cubic lattice was first introduced by Elliott.[2] The competing effect along the anisotropic direction was determined by K, the ratio of the second to the first neighbor interactions. The main characteristics of the phase diagram (in the space of temperature T and $K=J_2/J_1$) are the occurrence of a Lifshitz point at $K<\frac{1}{2}$,[3,4,5] an

[1] Department of Materials Science and Mineral Engineering, Berkeley, California 94720.
[2] Permanent Address: ONERA, BP72, 92322 Chatillon Cedex, France.

0022-4715/86/0500-0645$05.00/0

incommensurate phase,[6] an infinite countable series of commensurate phases springing from a multiphase point,[7,8] and a branching process.[9]

Much attention has been paid to the 2-d ANNNI model since it presents a rather different picture. The most interesting feature is the nature of the incommensurate phase. On the basis of Monte Carlo simulations,[10] it was suggested that the transition between this phase and the disordered one had an X–Y character, dislocation-like spin configurations playing the role of the vortices of the Kosterlitz–Thouless theory.[11] Using this idea and a free fermion approximation, Villain and Bak[12] showed that the incommensurate phase is a floating phase, characterized by algebraically decaying correlation functions. The unbinding of the dislocation-like configurations drives the transition to the disordered phase, which is stable down to $T=0$. This last result is confirmed by an analogy with a quantum Hamiltonian[13] and an exact calculation along one line of the phase diagram.[14] Previous Monte-Carlo results[10,5] suggesting the occurrence of a Lifshitz point at finite temperature for $K<\frac{1}{2}$ were shown to be due to finite size effects.[16] On the other hand, the existence of a Lifshitz point at a finite value of $K>\frac{1}{2}$ has been proposed[17] and can be derived from the free fermion approximation.[12,16] However, the possibility that the transition between the incommensurate phase and the disordered one extends to $K=\infty$ has been suggested,[18] thereby rejecting the Lifshitz point to $K=\infty$.[19]

In this article, we attempt to calculate a complete phase diagram using only one technique, the cluster variation method. We confirm the stability of the disordered phase down to $T=0$, and the absence of a Lifshitz point at finite temperature for $K<\frac{1}{2}$. The existence of two regimes of modulations for the correlation functions inside the disordered phase leads us to the determination of a "disorder" line. The study in reciprocal space of the stability of the disordered phase allows us to define a critical line in the phase diagram along which the q vector characterizing the instability is incommensurate. Finally, we show that the Lifshitz point for $K>\frac{1}{2}$ occurs at $K=\infty$.

2. THE TWO-DIMENSIONAL ANNNI MODEL AND THE CVM

The model is described by the Hamiltonian

$$\mathscr{H}=\sum_{x,y}\left(J_0\sigma_{x,y}\sigma_{x,y+1}+J_1\sigma_{x,y}\sigma_{x+1,y}+J_2\sigma_{x,y}\sigma_{x+2,y}\right) \tag{1}$$

where the spins $\sigma_{x,y}$ ($=\pm 1$) are located on the sites of a rectangular lattice with the lattice constant a in the x direction. The coupling along the y direction is ferromagnetic ($J_0<0$) while, along the x direction, there is a

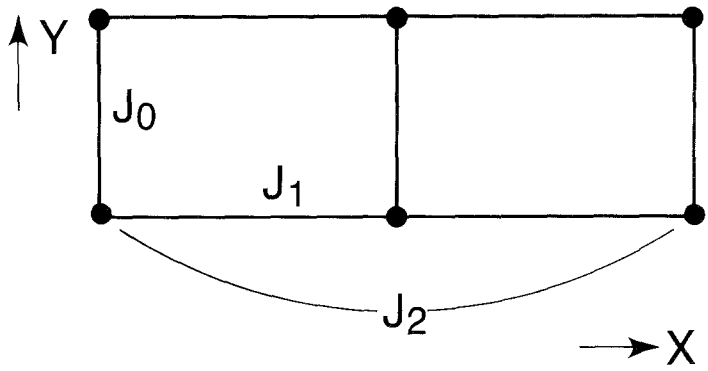

Fig. 1. The two-dimensional ANNNI model.

competition between antiferromagnetic first- and second-neighbor interactions ($J_1 > 0$ and $J_2 > 0$) (Fig. 1). We consider $J_0 = -J_1$. The competing effect along the anisotropic direction is measured by $K = J_2/J_1$. Since the coupling along the y direction is ferromagnetic, the y chains in an ordered phase will be predominantly ferromagnetically ordered. Hence, an ordered phase is completely defined by the sequence of predominantly up and down y chains along the x direction. In what follows, a commensurate phase is denoted by Fisher and Selke's notation: for example, the sequence $++-++-,...$ is represented by $\langle 21 \rangle$, in which the brackets indicate a repeating period (or half-period), see Fig. 2. A domain of size n is a sequence of n consecutive y chains with the same predominant magnetization (say $+$) preceded and followed by y chains with the opposite magnetization ($-$). We denote by M the mean value of the domain size. Thus, for a commensurate phase, we obtain $M = p/q$, where p is the number of y chains and q the number of domains involved in the period (or half period) of the commensurate phase. The ground state for

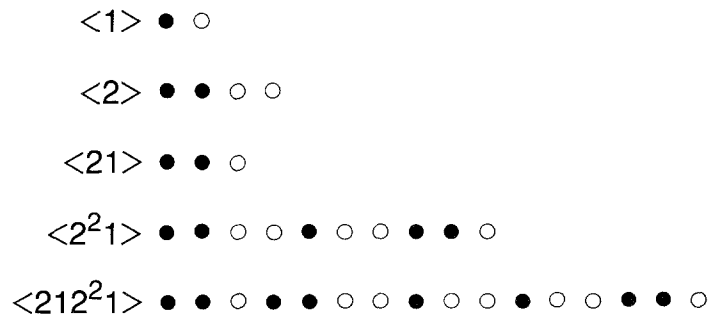

Fig. 2. Ordered commensurate phase considered in this study.

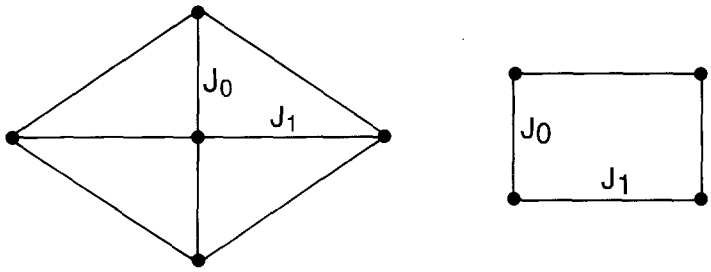

Fig. 3. Clusters used for the CVM approximation. Rectangular cluster suggested by R. Kikuchi.

$K<\frac{1}{2}$ is antiferromagnetic, noted $\langle 1\rangle$, and goes over, for $K>\frac{1}{2}$ to a $\langle 2\rangle$ antiphase state. The point $K=\frac{1}{2}$ is infinitely degenerate: all phases which do not contain more than two consecutive chains of up (down) spins are stable. The phase diagram presented in the next section has been obtained by using the cluster variation method (CVM).[20] The approximate CVM entropy was determined by using two clusters: centered lozange and rectangle (Fig. 3).[3] The accuracy of the CVM can be estimated by the results at the particular value $K=0$ for which the ANNNI model reduces to the Onsager Ising model: the CVM critical temperature turns out to be only 4% above that of the exact result. The CVM has also been proven to be reliable for two-dimensional models by the comparison of a CVM analysis and the exact solution of a different ANNNI model, the uniaxial brickwork lattice.[22]

3. PHASE DIAGRAM

A CVM study of a phase diagram consists essentially of comparing the free energies of a certain number of different phases. For any point of the phase diagram, the equilibrium state is determined by the phase with the lowest free energy among those which have been considered in the study. This implies that an infinite number of phases should be taken into account, which is obviously impossible. Hence, the first step is to specify a priori which phases are likely to be stable in some region of the phase diagram in the plane $(k_B T/|J_0|, K)$. The first candidates are naturally the ground states $\langle 1\rangle$ and $\langle 2\rangle$. Since the point $(K=\frac{1}{2}, T=0)$ is infinitely degenerate, we should expect that entropy effects might lift the degeneracy between the phases stable at this point. In the three-dimensional version of the ANNNI model, a low temperature expansion around this point has indeed proved that an infinite number of commensurate phases spring from

[3] The choice of these clusters was proposed by R. Kikuchi and J. Kulik.

the multiphase point.[7,8] In the case where J_1 is antiferromagnetic, this infinite countable sequence is represented by the basic phases $\langle 2^j 1 \rangle$, with $j = 1, 2, 3, \ldots$. This provides us with a second set of phases possibly stable around the multiphase point.

We have performed a first CVM analysis with the phases $\langle 1 \rangle$, $\langle 2 \rangle$, $\langle 21 \rangle$ (see Fig. 2) and the disordered phase. The resulting phase diagram is presented in Fig. 4. We note that, contrary to the three-dimensional case, the disordered phase is stable down to the multiphase point at $T = 0$ (at least down to $k_B T/|J_0| = 0.4$; it is difficult to reach a CVM equilibrium state for lower temperatures because of poor numerical convergence). As a second step, we have introduced the next basic phase, $\langle 2^2 1 \rangle$ (see Fig. 2). According to the three-dimensional case, and because this structure is a mixture of $\langle 21 \rangle$ and $\langle 2 \rangle$, we expect this phase to be stable between the $\langle 21 \rangle$ and $\langle 2 \rangle$ phases. As can be seen from Fig. 4, this is effectively the case: the previous common boundary between $\langle 21 \rangle$ and $\langle 2 \rangle$ disappears and is replaced by the stability regions of the $\langle 2^2 1 \rangle$ at the expense of $\langle 21 \rangle$ and $\langle 2 \rangle$, the stability region of which are decreased in extent. Note that both phases $\langle 21 \rangle$ and $\langle 2^2 1 \rangle$ are stable down to the multiphase point. We may anticipate that the same qualitative result will be obtained in the

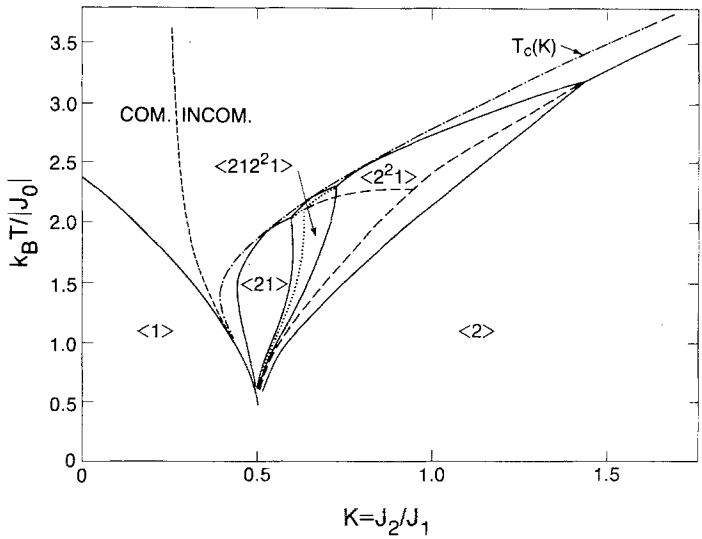

Fig. 4. Phase diagram of the two-dimensional ANNNI model. Full lines represent the complete phase diagram with phases $\langle 1 \rangle$, $\langle 2 \rangle$, $\langle 21 \rangle$, $\langle 2^2 1 \rangle$ and $\langle 212^2 1 \rangle$. Previous stages in the calculation are shown by broken lines ($\langle 1 \rangle$, $\langle 2 \rangle$, $\langle 21 \rangle$) and dotted lines ($\langle 1 \rangle$, $\langle 2 \rangle$, $\langle 21 \rangle$, $\langle 2^2 1 \rangle$). The dot-dashed line represents the curve $T_c(K)$ and the dashed line the "disorder" line.

vicinity of the boundary $\langle 2^2 1 \rangle \langle 21 \rangle$ by considering the next basic phase $\langle 2^3 1 \rangle$. In fact, this process could be repeated indefinitely: each new phase $\langle 2^j 1 \rangle$ will stabilize between and at the expense of the phases $\langle 2^{j+1} 1 \rangle$ and $\langle 2 \rangle$.

A third set of structures which could be stable is provided by the so-called branching process. In the 3-d ANNNI model, a mean field approach[9] has shown that two adjacent basic phases, say $\langle 21 \rangle$ and $\langle 2^2 1 \rangle$ (or A and B) are separated, beyond a branching point (K_b, $T_b > 0$), by the simple combination structure $\langle 212^2 1 \rangle$ (or AB). At another branching point, the boundary between A and AB may become unstable against the higher-order combination AAB. This process, repeated ad infinitum, can be represented by a graph, in fact a rooted tree with an infinite number of branches springing from branching points at finite temperature.[23] The trunk separates the two basic structures which characterize the tree and each branching point is the origin of a branching phase. Such a graph can be associated with any pair of consecutive basic structures $\langle 2^j 1 \rangle$, $\langle 2^{j+1} 1 \rangle$. If M_A and M_B are the mean domain-sizes of the commensurate phases A and B, all the rational numbers between M_A and M_B are generated as the branching process is repeated. We have considered only the simplest branching phase, $\langle 212^2 1 \rangle$ (see Fig. 2). (In the CVM approximation used in this study, the free energy of this phase is obtained by minimizing a functional of 155 independent correlation functions.) The resulting phase diagram is presented in Fig. 4. The transition between any ordered phase and the disordered one is of second order, whereas the transition between ordered phases is of first order. As expected, the $\langle 212^2 1 \rangle$ phase is stable between $\langle 21 \rangle$ and $\langle 2^2 1 \rangle$. However, unlike the three-dimensional case, the branching point seems to fall down to the multiphase point ($K = \frac{1}{2}$, $T = 0$). There is no reason to believe that this result would not generalize to any branching phase. Hence, for any fixed value of T (sufficiently low), M takes all the rational values as a function of K, in the wedge between the $\langle 1 \rangle$ and $\langle 2 \rangle$ phases. Thus, an approximate account of the branching process for the second ANNNI model could be presented as follows.

All the branching points of the tree associated to any two consecutive basic phases fall down to the multiphase point, which becomes the origin of an infinite number of branches of all the trees, in such a way that any phase, basic or resulting from a branching combination, sees its stability region reduced to a single line. As a result, the wedge between the $\langle 1 \rangle$ and $\langle 2 \rangle$ phases would be filled up by an infinite number of transition lines between stability regions reduced themselves to lines. Only commensurate phases are involved in this process. Hence, at fixed T, M, the mean value of the domain size, should take, as a function of K, only rational values.

However, the set of rationals has measure zero in the set of real numbers. Thus, if each rational value of M occurs only for one value of K, the set of K values for which a commensurate phase is stable should have measure zero. As a result, irrational values of M should be found almost everywhere, as proved by a low temperature analysis.

Indeed, a low temperature expansion of the 2-d ANNNI model has been carried out using a free fermion approximation.[12] The most interesting result obtained by this method is the occurrence of a floating phase in the wedge between the $\langle 1 \rangle$ and $\langle 2 \rangle$ phases. Analytically, the floating phase is characterized by algebraically decaying correlations.[24] Along the x direction, the pair correlation function is given by

$$\zeta(\mathbf{R}) \simeq |\mathbf{R}|^{-\eta} \cos \mathbf{q}_0 \cdot \mathbf{R}$$

where $\mathbf{R}$ is a lattice vector and $\mathbf{q}_0$ a wave vector which defines the modulation in the floating phase. In all generality, the singular exponent, η, and $\mathbf{k}_0$ are functions of T and $K = J_2/J_1$. As a result of this algebraic decay, the floating phase presents no long-range order. The wave vector $\mathbf{k}_0$, related to the inverse of M, is found to be incommensurate. Since power law decay is usually associated with critical points, we can in some sense regard a floating phase as being always in a critical regime. However, since the floating phase is essentially incommensurate, to account for this phase in terms of the ultimate limit of an infinite set of commensurate phases offers only a qualitative picture.

In the CVM framework, the only way of dealing with the incommensurate aspect of a phase is to transcribe the formalism into reciprocal space. Actually, the CVM free energy of any phase is expressed as a function of correlation parameters which are defined by the symmetries of the phase. In particular, if there is no periodicity, as in the case of an incommensurate phase, the number of correlation functions is infinite, preventing us from computing the free energy. It is then of interest to study the susceptibility $\chi(q)$ of the disordered phase in q space. More precisely, the disordered phase is unstable when the susceptibility diverges and the q vector where this divergence occurs characterizes the modulation of the phase which destabilizes the disordered one. In particular, the nature of the q vector (rational or irrational) defines the nature of the phase (commensurate or incommensurate).

4. SUSCEPTIBILITY $\chi(q)$

As mentioned above, an effective way of carrying out the CVM is to study the susceptibility $\chi(q)$ in q space. The formalism will be briefly summarized below; for more details, the reader is referred to Refs. 25 and 28.

In all generality, the CVM free energy can be expressed as the minimum of

$$F = E\{\xi\} - TS\{\xi\} \tag{2}$$

where the internal energy functional is given by

$$E\{\xi\} = \sum_{\alpha} h_\alpha \xi_\alpha \tag{3}$$

and the configurational entropy functional is given by

$$S\{\xi\} = -k_B \sum_{\alpha} a_\alpha \operatorname{Tr} \rho_\alpha \ln \rho_\alpha \tag{4}$$

In these equations, k_B and T have their usual meaning, $\xi_\alpha(R)$ is a multisite correlation function for a cluster of n_α points centered on lattice point R, h_α is a corresponding interaction energy, the set a_α are positive or negative integers which depend on the type of cluster and on the crystal structure, ρ_α are reduced density matrices, i.e., they represent the probability of finding cluster α in a given configuration, the trace Tr being interpreted as a sum over allowed configurations. The a priori probability of occurrence of a given configuration is $\rho_\alpha^* = \frac{1}{2^{n_\alpha}}$ for a binary system, i.e., one for which lattice site occupancy is determined by the spin variable $\sigma(\mathbf{R}) = \pm 1$. Density matrices and correlations are related by

$$\rho_\alpha = \rho_\alpha^* \left[1 + \sum_{\beta \subset \alpha} \sigma_\beta \xi_\beta \right] \tag{5}$$

with

$$\sigma_\beta = \prod_{\mathbf{R} \in \beta} \sigma(\mathbf{R})$$

In (5) the sum extends over all subclusters (β) of the cluster (α) considered.

By (2)–(4) the free energy F can be considered formally as a function of the $\{h_\alpha\}$, and hence can be regarded as the Legendre transform of $-TS(\xi)$, the parameters h_α then appearing as field variables conjugate to the variables ξ_α. Indeed, the minimization condition

$$\frac{\partial F}{\partial \xi_\alpha} = 0 \qquad (\text{all } \alpha) \tag{6}$$

leads directly to the equilibrium condition

$$h_\alpha = \frac{\partial (TS)}{\partial \xi_\alpha} \tag{7}$$

It is also seen that the second derivatives $F_{\alpha\beta}$ of F with respect to ξ_α, ξ_β are given explicitly by

$$F_{\alpha\beta} = -\frac{\partial^2(TS)}{\partial\xi_\alpha\,\partial\xi_\beta} = kT \sum_{\substack{\gamma\supset\alpha \\ \gamma\supset\beta}} a_\gamma \,\mathrm{Tr}(\rho_\gamma^*)^2 \frac{\sigma_\alpha\sigma_\beta}{\rho_\gamma} = -\frac{\partial h_\alpha}{\partial\xi_\beta} \tag{8}$$

The matrix inverse to $F_{\alpha\beta}$ can be regarded as a generalized susceptibility matrix $\{\chi_{\alpha\beta}\}$ with

$$\chi_{\alpha\beta}(\mathbf{R}) = -\frac{\partial\xi_\beta(\mathbf{R})}{\partial h_\alpha}$$

in which the $\mathbf{R}$ dependence of the correlations, and hence of the susceptibility, has been indicated.

The matrix $\{F_{\alpha\beta}(\mathbf{R})\}$ can be Fourier-transformed along with the susceptibility matrix, yielding

$$\{\chi_{\alpha\beta}(\mathbf{q})\} = \{F_{\alpha\beta}(\mathbf{q})\}^{-1} \tag{10}$$

By the fluctuation dissipation theorem, the first diagonal element χ_{11} of the q space susceptibility matrix is proportional to the Fourier transform of the pair correlation function (short-range order intensity in the diffractionists' terminology).[25] Attention will now be focused on this element, henceforth referred to as *the* susceptibility $\chi(\mathbf{q})$, for short.

A second-order transition between the disordered phase and an ordered one is characterized by the divergence of the susceptibility $\chi(\mathbf{q})$ for the q vector which determines the periodicity of the ordered phase. The basic method of studying $\chi(\mathbf{q})$ is as follows: At fixed K, starting from high temperature in the disordered phase, we look for the q vector $q_M(K, T)$ where $\chi(q)$ takes its maximum value (only one component of the full wavevector needs to be considered, since there is competition only along the x axis). Then we follow the variation of $q_M(K, T)$ as T is lowered, keeping K fixed. We present in Fig. 5 some curves $\chi(q)$ for various temperatures at $K = 0.4$. We note that as T is decreased the maximum of the susceptibility increases and that $q_M(K, T)$ varies continuously and eventually locks-in at $q = 0.5$, the value of the q vector which characterizes the modulation of the $\langle 1 \rangle$ phase. If we continue to decrease T, $q_M(K, T)$ stays locked at 0.5 and the maximum of $\chi(q)$ continues to increase and eventually diverges. We found a similar result for any value of K between 0.25 and 0.5 (see the example in Fig. 6 for $K = 0.3$). As a result, there exist two different regimes in the disordered phase separated by a "disorder line" defined by the lock-in transition of $q_M(K, T)$ (see Fig. 4). Above and to the "right" of this line, the q value where $\chi(q)$ is maximum varies continuously with T and K,

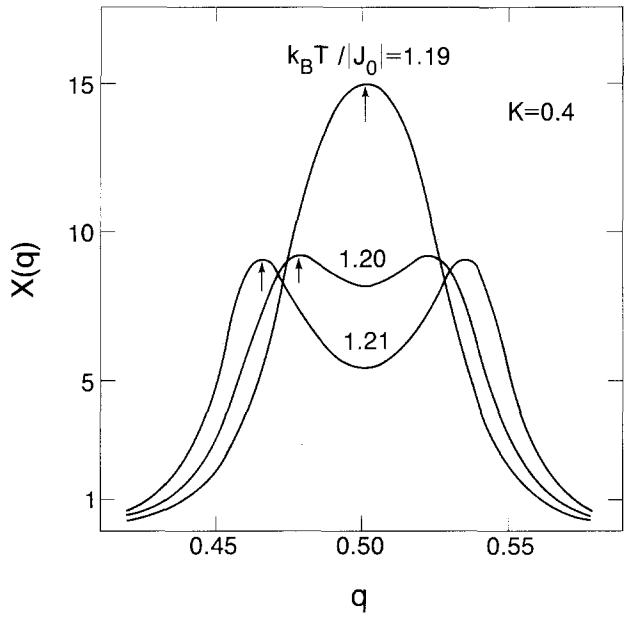

Fig. 5. Temperature dependence of the susceptibility $\chi(q)$ for $K=0.4$. The wave-vector q is measured in units of $2\pi/a$ and $\chi(q)$ in arbitrary units. The arrows indicate the location of the maxima of the susceptibility.

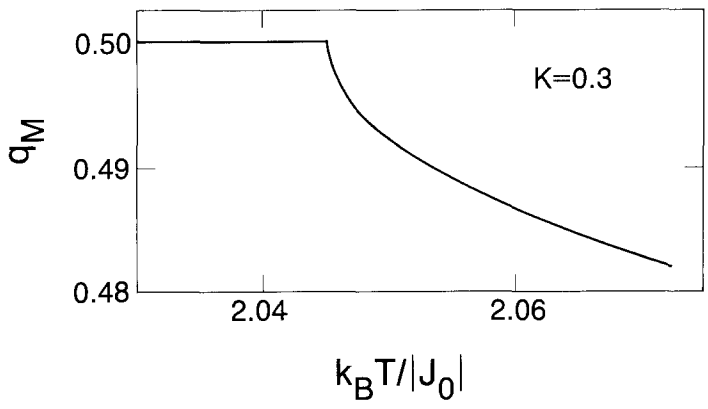

Fig. 6. Temperature dependence of q_M, the wave vector where the susceptibility is maximum, for $K=0.3$. q_M is measured in units of $2\pi/a$.

being then incommensurate with the lattice almost everywhere. This region reflects, then, the existence of competition between the interactions J_1 and J_2 which tends to favor incommensurate modulations, at least at high temperature. Under the disorder line, $q_M(K, T)$ locks-in at 0.5, reflecting the natural periodicity imposed by the lattice and J_1, at low temperature and small $K = J_2/J_1$. In this region, the maximum of the susceptibility is still finite but increases as T decreases and eventually diverges at a temperature which is exactly equal to the transition temperature of the $\langle 1 \rangle$ phase found in the real space analysis, in agreement with the fact that the divergence occurs at $q = 0.5$, corresponding to the modulation of the $\langle 1 \rangle$ phase. This, in turn, confirms the second-order character of the transition. Thus the only instability of the disordered phase under the disorder line corresponds to the transition to the $\langle 1 \rangle$ phase. We note that the disorder line goes down to the point $K = 0.5$, $T = 0$. These results prove without ambiguity that the disordered phase is stable down to the multiphase point.

We present in Fig. 7 the results of the susceptibility analysis for

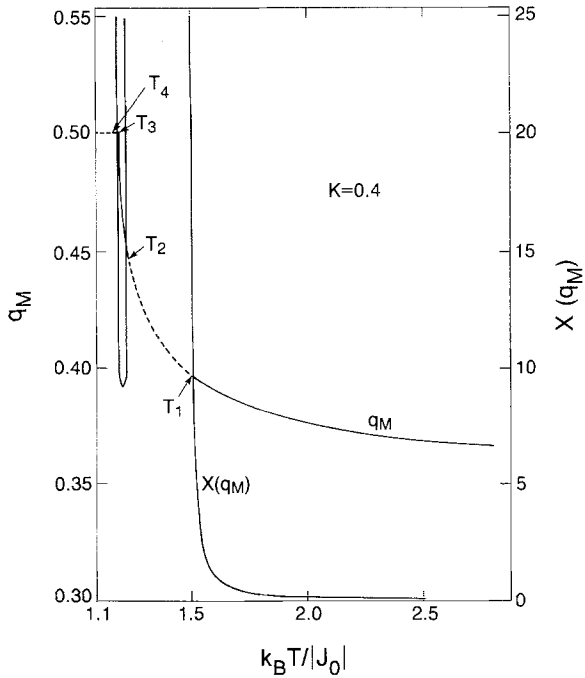

Fig. 7. Temperature dependence of $\chi(q_M)$, maximum of the susceptibility, and q_M, q vector where this maximum occurs, for $K = 0.4$. q_M is measured in units of $2\pi/a$, $\chi(q_M)$ in arbitrary units. The susceptibility diverges at $k_B T_1/|J_0| = 1.496$, stays infinite until the temperature reaches $k_B T_2/|J_0| = 1.236$. The lock-in transition occurs at the $k_B T_3/|J_0| = 1.193$, and the transition to the $\langle 1 \rangle$ phase at $k_B T_4/|J_0| = 1.175$.

$K=0.4$. We remark that the susceptibility diverges first at a high temperature $k_B T_1/|J_0| = 1.496$ and that the q value where this divergence occurs is incommensurate. This latter remark is based on the fact that the q value where $\chi(q)$ is maximum is a smooth (differentiable) function of T (see Fig. 7). As T decreases, the susceptibility stays infinite until the temperature reaches the value $k_B T_2/|J_0| = 1.236$ and finally becomes finite again below the temperature T_2 at which the susceptibility also diverges at an incommensurate value of q. According to the argument presented above, this indicates that the disordered phase is unstable between T_1 and T_2 and stable again under T_2. As T continues to decrease, we recover the previous features: $q_M(K, T)$ varies continuously and locks-in at $q=0.5$ for $k_B T_3/|J_0| = 1.193$ while the maximum of the susceptibility, after first decreasing, increases and finally diverges for $k_B T_4/|J_0| = 1.175$, the transition temperature of the $\langle 1 \rangle$ phase. The instability of the disordered phase between T_1 and T_2 cannot be seen in the real space analysis (see Fig. 4), since the q vectors where the susceptibility diverges at T_1 and T_2 are incommensurate.

To summarize the results of the susceptibility analysis, we note, for any value of K, the temperature $T_c(K)$ where the maximum of the susceptibility of the disordered phase diverges (see Fig. 4) and $q_c(K)$, the q vector where this divergence occurs (Fig. 8). Each of these curves is divided into two segments by the multiphase point; without ambiguity, we can say that one segment lies on the $\langle 1 \rangle$ side of the phase diagram and the other on the $\langle 2 \rangle$ side. From the above results, we conclude that, on the $\langle 1 \rangle$ side of the

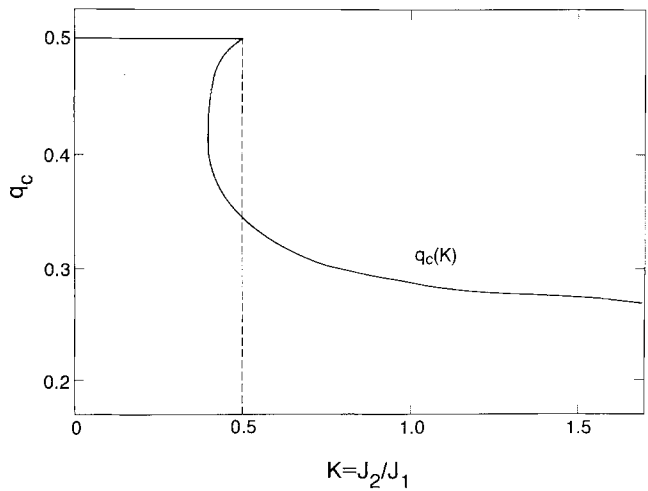

Fig. 8. Critical wave vector $q_c(K)$ in units of $2\pi/a$.

phase diagram, the curve $T_c(K)$ marks the transition to the $\langle 1 \rangle$ phase and goes down to the point $K=\frac{1}{2}$, $T=0$ where it meets the disorder line. Along the corresponding segment, $q_c(K)$ is locked at $q=0.5$. On the $\langle 2 \rangle$ side, we found that $T_c(K)$ lies always above the phase boundaries determined by the real space analysis. More precisely, $T_c(K)$ has only one common point with each commensurate phase. At this point, the curve $T_c(K)$ is tangent to the boundary of the commensurate phase and $q_c(K)$ is exactly equal to the characteristic wave vector of the modulation of this phase, in agreement with the observation in the real space analysis of a second-order transition between any ordered phase and the disordered one. We note that the curve $q_c(K)$ is a smooth continuous function of K. Hence, the equilibrium state, along the corresponding segment of $T_c(K)$, is incommensurate almost everywhere.

Another interesting question is whether there is a direct transition between the disordered phase and the $\langle 2 \rangle$ phase beyond some value of the parameter K, which would indicate the existence of a Lifshitz point on the $\langle 2 \rangle$ side of the phase diagram. The occurrence of this point has been suggested in the Hamiltonian limit[17] and can be derived from the free fermion approximation.[12] However, the possibility of a thin tongue of incommensurate phase above the $\langle 2 \rangle$ phase extending to $K=\infty$ has not been completely ruled out.[18] In order to address this question, we have used another set of interaction parameters

$$\frac{J_1}{|J_0|}=1-\alpha, \qquad \frac{J_2}{|J_0|}=\alpha$$

which allows us to reach the limit $K=\infty$ for the finite value $\alpha=1$. The phase diagram in the plane $(k_BT/|J_0|, \alpha)$ cannot be obtained from the one in the plane $(k_BT/|J_0|, K)$ by simply applying a scaling factor along the K axis since, in the latter case, the ratio J_1/J_0 was kept fixed. In Fig. 9, we present the curves $T_c(\alpha)$ (Fig. 9a) and $q_c(\alpha)$ (Fig. 9b) obtained by the susceptibility analysis. The curve $q_c(\alpha)$ is a smooth continuous function of α which goes down to $q=\frac{1}{4}$ and reaches this value only for $\alpha=1$. This result proves that the Lifshitz point on the $\langle 2 \rangle$ side of the phase diagram occurs at $\alpha=1$, where the first-neighbor pair interaction J_1 vanishes. Therefore, the Lifshitz point merges with the "decoupling" point[19] where the ANNNI model reduces to two independent Onsager lattices.

5. DISCUSSION AND SUMMARY

On the $\langle 1 \rangle$ side, we found that the first instability of the disordered phase corresponds to the second-order transition of the $\langle 1 \rangle$ phase, the

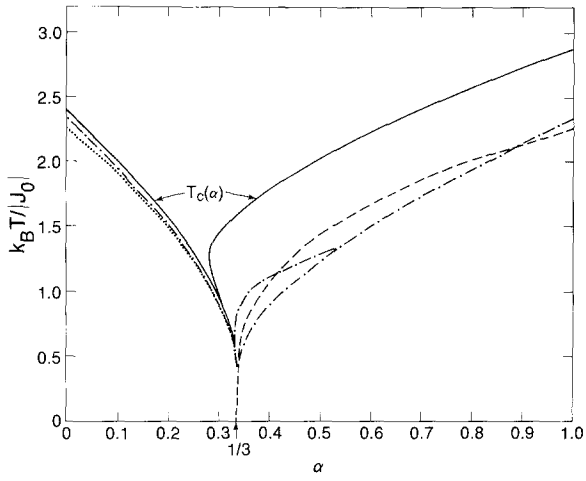

(a)

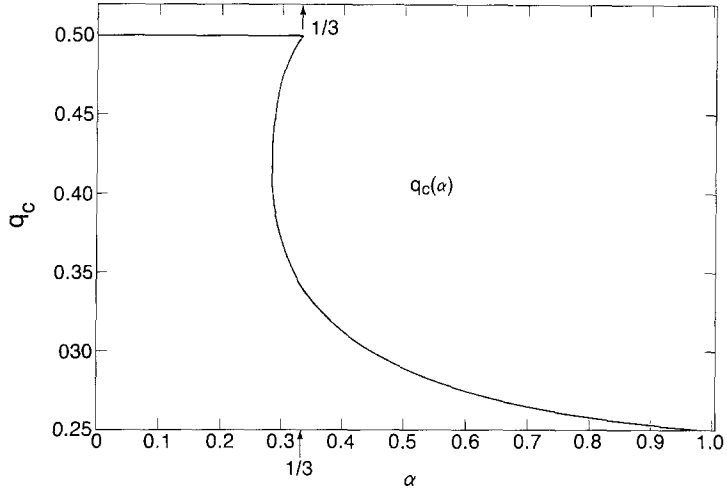

(b)

Fig. 9. (a) Critical lines $T_c(\alpha)$. Also presented are the transition temperature of the $\langle 1 \rangle$ phase calculated by the Müller–Hartmann and Zittartz method (dotted line), of the $\langle 2 \rangle$ phase determined by the Pesch and Kroemer method (dashed line), and the phase diagram obtained by the free fermion approximation (dot–dashed lines). (b) Critical wave vector $q_c(\alpha)$ in units of $2\pi/a$.

boundary of which goes down to the multiphase point. This implies, in turn, the stability of the disordered phase down to this point, in agreement with the results of Ref. 12, 13, 14, and 18. Inside the disordered phase, the lock-in transition of $q_M(K, T)$, the q vector where the susceptibility reaches its maximum, has been studied. The corresponding "disorder line" is asymptotically tangent to the line $K=0.25$ and goes down to the multiphase point. Note that this line approaches the boundary of the $\langle 1 \rangle$ phase around $K=0.35$ and follows it very closely, but separated, down to the multiphase point. This feature has been speculated[16] to account for the observation of a Lifshitz point in previous Monte Carlo calculations.[10,15] The results presented here exclude the existence of a Lifshitz point at finite temperature along the boundary of the $\langle 1 \rangle$ phase. More precisely, and according to its definition,[3] the Lifshitz point merges with the multiphase point, since a critical curve, along which the modulation q varies continuously, arises from this point. Indeed, on the $\langle 2 \rangle$ side of the phase diagram, the instability of the disordered phase has been characterized by the critical line $T_c(K)$ along which the critical wave vector $q_c(K)$ is incommensurate with the underlying lattice almost everywhere. Moreover, the line $T_c(K)$ appears to be an envelope curve of the boundaries of the commensurate phases introduced in the real space analysis. These results do not disagree with the occurrence of a floating phase. As explained above, the observed stability of commensurate phases is only a metastable effect. Finally, the study of the instability of the disordered phase as $J_1 \to 0$ ($\alpha \to 1$) proved the existence of a Lifshitz point on the $\langle 2 \rangle$ side of the phase diagram at $\alpha = 1$.

The CVM results can be compared with those obtained by other methods. The phase boundary of the $\langle 1 \rangle$ phase can be obtained by using the method of Müller–Hartmann and Zittartz[26,16] and the free fermion approximation.[12] The agreement of these two results, as well as with Monte Carlo simulations[10,16] is very good, especially near the multiphase point (see Fig. 9a). On the $\langle 2 \rangle$ side of the phase diagram, the curve $T_c(K)$ presented here lies above the results obtained by the free fermion approximation, the method of Pesch and Kroemer,[27] and the Monte Carlo simulation. In fact, we expect the CVM results to be less accurate as J_2 increases, since the size along the x axis of the largest cluster used to approximate the entropy (Fig. 3) is precisely equal to the distance between second neighbors. For $J_1 = 0$, the CVM approximation used here reduces to a second-neighbor pair in the x direction and a linear triplet along the y axis. Therefore, the CVM accuracy is reduced. For example, for $J_1 = 0$ ($\alpha = 1$), where our model reduces to an Onsager lattice, the precision on T_c is only 25%. Another important remark is that the floating incommensurate phase is characterized by algebraically decaying correlation

functions reflecting large fluctuations and the absence of a correlation length. Therefore, the CVM, which is a mean field theory where the units embedded in a mean field are the chosen clusters, cannot describe accurately the critical regime which precedes the transition toward the floating phase. However, our results prove that the disordered phase is stable down to $T=0$, whereas the usual mean field theory would predict the existence of a Lifshitz point on the boundary of the $\langle 1 \rangle$ phase for $K=0.25$. The stability of the disordered phase down to the multiphase point is a consequence of the X–Y-like behavior of the floating phase. Dislocation-like spin configurations[10,12,16] play the role of the vortices of the Kosterlitz–Thouless theory.[11] The unbinding of these dislocations is responsible for the transition of the floating phase into the disordered phae. Thus, the the CVM approximation used here seems to treat quite well the essential physical features of the 2-d ANNNI model. Therefore, we believe that the results $T_c(K)$ and $q_c(K)$ [$T_c(\alpha)$ and $q_c(\alpha)$] are qualitatively correct. A comparison of a CVM analysis and the exact solution of a different two-dimensional model, the uniaxial brickwork lattice, confirms this point of view.[22]

ACKNOWLEDGMENTS

The authors have benefitted from helpful conversations with F. Ducastelle, A. D. Haymet, J. Kulik, W. Selke, and J. Yeomans and especially thank R. Kikuchi for having suggested the use of the rectangular cluster in the CVM approximation. This work was supported by the Director, Office of Energy Research, Office of Basic Energy Sciences, Materials Sciences Division of the U. S. Department of Energy under Contract Number DE-AC03-76SF00098.

REFERENCES

1. W. Selke, in *Nato Advanced Study Institute on Modulated Structure Materials*, T. Tsakalakos, ed. (Maleme-Chania, Crete, 1983).
2. R. J. Elliott, *Phys. Rev.* **124**:346 (1961).
3. R. M. Hornreich, M. Luban, S. Shtrikman, *Phys. Rev. Lett.* **35**:1678 (1975); R. M. Hornreich, M. Luban, S. Shtrikman, *Phys. Rev.* **B19**:3799 (1979).
4. R. M. Hornreich, *J. Magn. Magn. Mater.* **15–18**:387 (1980).
5. S. Redner and H. E. Stanley, *Phy. Rev.* **B16**:577 (1977).
6. J. von Boehm and P. Bak, *Phy. Rev. Lett.* **12**:122 (1979); P. Bak, J. von Boehm, *Phy. Rev.* **B21**:5297 (1980).
7. M. E. Fisher and W. Selke, *Phy. Rev. Lett.* **44**:1502 (1980). M. E. Fisher and W. Selke, *Philos. Transact. Soc.* **302**:1 (1981).
8. V. L. Pokrovskii and G. V. Uimin, *Zh. Eksp. Teor. Fiz* **82**:1640 (1982).

9. P. M. Duxbury and W. Selke, *J. Phys.* **A16**:L741 (1983); W. Selke and P. M. Duxbury, *Z. Phys.* **B57**:49 (1984).
10. W. Selke and M. E. Fisher, *Z. Physik* **B40**:71 (1980).
11. J. M. Kosterlitz and D. J. Thouless, *J. Phy.* **C6**:1181 (1973); J. M. Kosterlitz and D. J. Thouless, *J. Phys.* **C7**:1046 (1974).
12. J. Villain and P. Bak, *J. Physique* **42**:657 (1981).
13. P. M. Duxbury and M. N. Barber, *J. Phys.* **A15**:3219 (1982).
14. I. Peschel and V. J. Emergy, *Z. Phys.* **B43**:241 (1981).
15. R. M. Hornreich, R. Liebmann, H. G. Schuster and W. Selke, *Z. Phys.* **B35**:91 (1979).
16. W. Selke, *Z. Phys.* **B43**:335 (1981).
17. M. N. Barber and P. M. Duxbury, *J. Phys.* **A14**:L251 (1981).
18. P. Rujan, *Phys. Rev.* **B24**:6620 (1981).
19. D. A. Huse and M. E. Fisher, *J. Phys.* **C15**:L585 (1982).
20. R. Kikuchi, *Phys. Rev.* **81**:998 (1951).
21. A. Finel and D. de Fontaine, *J. Stat. Phys.* **43**:663 (1986).
22. D. de Fontaine, *J. Phys. A: Math. Gen.* **17**:L713 (1984).
23. D. R. Nelson and B. I. Halperin, *Phys. Rev.* **B19**:2457 (1979).
24. J. M. Sanchez, *Phys. A* **111**:200 (1982).
25. E. Mülluer–Hartmann and J. Zittartz, *Z. Phys.* **B27**:261 (1977).
26. J. Kroemer and W. Pesch, *J. Phys.* **A15**:L258 (1982).
27. J. M. Sanchez, F. Ducastelle, and D. Gratias, *Phys. A* **128**:334 (1984).